applied sciences

MDPI

Article

Mechanical and Tribological Performance of Carbon Fiber-Reinforced PETG for FFF Applications

Moises Batista [1], Jose Miguel Lagomazzini [1], Magdalena Ramirez-Peña [1] and Juan Manuel Vazquez-Martinez [2,*]

[1] Mechanical Engineering and Industrial Design Department, School of Engineering, University of Cadiz, Avda. de la Universidad de Cadiz, 10, E11519 Puerto Real, Spain; moises.batista@uca.es (M.B.); josemiguel.lagomazzinicaballero@alum.uca.es (J.M.L.); magdalena.ramirez@uca.es (M.R.-P.)

[2] Industrial Engineering and Civil Engineering Department, Polytechnic School of Engineering of Algeciras, Avda. Ramón Puyol, s/n, E11202 Algeciras, Spain

* Correspondence: juanmanuel.vazquez@uca.es; Tel.: +34-956483513

Abstract: With the increasing adoption of Additive Manufacturing in the industry, driven by its efficiency, productivity, and project profitability, materials have undergone significant evolution to enhance process performance and part properties. One of the processes employed to enhance these properties involves the incorporation of various types of reinforcements. This aims to ensure that the material acquires a proportion of the properties of the added reinforcement. Consequently, the options for material selection expand depending on the application. Hence, there is a need to understand how specific reinforcements modify the properties of these materials. For this reason, this study investigates the modification of mechanical properties in a PETG matrix through the incorporation of short carbon fiber (CF) reinforcements, driven by their industrial relevance. To achieve this, the Fused Filament Fabrication (FFF) process will be utilized to produce a series of standardized specimens made of both PETG and CF-reinforced PETG, with variations in layer height and extrusion temperature. Subsequently, these specimens will undergo mechanical evaluation in tension and compression, following the relevant standards for each case. Finally, distinctions between both materials will be analyzed, based on the data obtained from tensile and compression tests. The incorporation of carbon fiber reinforcement shows a detrimental effect, leading to a decrease in the material's stress (39.23 N/mm^2 vs. 48.41 N/mm^2 for the conventional material). As expected, due to the nature of the reinforcement (short fibers), the deformation of the material also decreases (2.13% compared to 2.9%).

Keywords: additive manufacturing; FFF; FDM; tensile test; pin on disc; PETG; reinforced material; CF; carbon fiber

check for updates

Citation: Batista, M.; Lagomazzini, J.M.; Ramirez-Peña, M.; Vazquez-Martinez, J.M. Mechanical and Tribological Performance of Carbon Fiber-Reinforced PETG for FFF Applications. *Appl. Sci.* **2023**, *13*, 12701. https://doi.org/10.3390/app132312701

Academic Editor: Mark J. Jackson

Received: 31 October 2023
Revised: 20 November 2023
Accepted: 24 November 2023
Published: 27 November 2023

Copyright: © 2023 by the authors. Licensee MDPI, Basel, Switzerland. This article is an open access article distributed under the terms and conditions of the Creative Commons Attribution (CC BY) license (https://creativecommons.org/licenses/by/4.0/).

1. Introduction

Additive Manufacturing (AM), also known as 3D printing, has emerged as a more sustainable alternative to traditional subtractive manufacturing in the industry. According to the F42 ASTM International Committee, additive manufacturing encompasses a set of processes that enable the layer-by-layer fabrication of physical objects from CAD models using materials of various compositions [1].

Among the techniques within Additive Manufacturing, Fused Filament Fabrication (FFF) is widely used. FFF employs a nozzle to melt filament material and progressively deposit it. Despite the extensive use of this method, ongoing efforts are dedicated to enhancing the quality of manufactured parts, reducing print times, and exploring new materials and applications. FFF primarily uses thermoplastic materials like polylactic acid (PLA), acrylonitrile butadiene styrene (ABS), polyethylene terephthalate glycol (PETG), nylon (Polyamide), or thermoplastic polyurethane (TPU) [2].

Carbon fiber as reinforcement may modify the surface finish of the developed parts. Several studies are focused on the improvement of the surface quality of the manufactured

parts, mainly due to the limitations of the printing process, and some post-processed methods are considered to improve the surface of the parts [3–7].

To improve their properties, especially their mechanical characteristics [8], some variations of these materials are reinforced with non-thermoplastic materials such as metals, ceramics, and synthetic or natural fibers. Among these, PETG is gaining prominence due to its minimal environmental impact. PETG, a modified PET copolymer, includes glycol to enhance flexibility, reduce moisture absorption, and provide transparency, making it suitable for FFF. However, the mechanical behavior of both materials becomes remarkably similar, differing mainly during flat deformation, where PET exhibits a more significant increase in strain, especially at 90 °C [9,10].

Below the glass transition temperature, these materials exhibit a distinctive yield point, followed by strain softening and moderate hardening at moderate strain levels, with substantial hardening occurring at large strains. Strain-induced crystallization plays a limited role under most strain conditions and predominantly affects the mechanical behavior during loading at higher strain levels in deformation conditions that result in the nearly uniaxial molecular orientation of the polymer structure [9,10]. However, compared to other materials used in FFF, such as PLA or ABS, PETG exhibits superior load-bearing capability [11]. Tensile tests indicate that PETG outperforms PLA and ABS, with a load of 2308 kN (0.077 kN/mm^2) compared to 2083 kN (0.053 kN/mm^2) and 1905 kN (0.049 kN/mm^2) for PLA and ABS, respectively. PETG also demonstrates the highest elongation percentage at 14.27%, compared to 5.263% and 8.772% for PLA and ABS, respectively [11]. Consequently, there is a growing interest in PETG for use in FFF, although the manufacturing of this material can be challenging. Despite the absence of common warping defects, manufacturing parameters play a crucial role in the process's performance. For example, the best mechanical properties for PETG were achieved at a 265 °C extruder temperature, 20 mm/s printing speed, 0.4 mm layer height, and 100% infill density [12]. Printing orientation significantly affects mechanical properties, particularly the elastic modulus and tensile strength [13]. A cross-axial orientation yields the highest fatigue strength, while the longitudinal orientation results in greater stiffness [13]. The material's performance is strongly influenced by the extrusion temperature. According to Hsueh et al. [14], as the printing temperature increases, so do the mechanical properties. This phenomenon has also been observed in other materials, such as PLA [14,15], although there is a threshold beyond which materials can degrade [15]. However, extrusion temperature is not the sole critical parameter; layer thickness also plays a crucial role in mechanical properties, significantly affecting tensile and compressive strength [16], as well as flexural strength [17,18]. This may be due to the fact that modifying the layer thickness affects the internal voids of the parts, altering their internal behavior [17], in line with the layer theory [19].

Moreover, reinforcing PETG with carbon fiber yields specific behaviors. According to Mansour et al. [20], the inclusion of carbon fibers in PETG results in a moderate reduction in damping capacity in alternating fatigue tests. This study concludes that the addition of carbon fiber significantly increases both the hardness and the elastic modulus of the material. Valvez et al. [21] also found that the inclusion of carbon fibers leads to increased displacements when compressive stresses are applied. Furthermore, tensile strength and stiffness are enhanced, although these outcomes are highly dependent on the orientation and deposition pattern [22].

PETG's attractive environmental performance has contributed to its increased interest. Regarding sustainability in PETG usage, some authors have thoroughly studied the material's recyclability, specifically the preservation or loss of mechanical properties after multiple recycling cycles. It has been determined that recycled PETG has a lower molecular weight than virgin PETG and lower tensile strength. Nevertheless, the flexural results of both materials are quite similar. The addition of continuous carbon fiber to the composite significantly enhances the properties of both materials, making the use of recycled PETG with added carbon fibers an appealing option from a sustainability perspective [23], even when using different concentrations of reinforcements [24].

Some systematic studies comparing the mechanical properties of parts produced with PETG and CF-reinforced PETG have been conducted; however, a reduced number of studies concerning the tribology of reinforcing materials with PETG has been detected [25–27]. Therefore, this study aims to examine the mechanical performance of parts produced with PETG and 20% CF-reinforced PETG, considering critical manufacturing parameters such as printing temperature and layer thickness. In addition, the printing limitations of PETG reinforced with carbon fiber have been studied based on the main effects in the use of PETG-CF filament on printing devices and the related defectology of printed parts. Finally, the tribological behavior resulting from the printing effects on the reinforced material has been evaluated by friction and wear analysis.

2. Materials and Methods

The experimental methodology used is shown in Figure 1.



Figure 1. Experimental Methodology flowchart.

2.1. Materials

To evaluate the mechanical properties, an experimental design based on mechanical tests was conducted to compare the behavior of a transparent PETG filament with a carbon-fiber-reinforced PETG filament (PETG-CF), both commercially available filaments with a diameter of 1.75 ± 0.02 mm. In this research, authors used short-fiber-reinforced PETG-CF (PETG CF Fibra de Carbono 1.75 mm) with a 20% CF percentage, from MÁSTONER (Madrid, Spain) supplier.

2.2. Methods

An XY Core kinematic 3D printer, Two Trees model Sapphire Plus (TwoTrees Technology, Shenzhen, China) with a generic brass nozzle of 0.4 mm diameter, was used for specimen fabrication. The specimen geometry was determined based on ASTM D638 [20] for the "bone-type" specimens and ASTM D695 [21] for the cylindrical specimens tested under compression. During this entire process, measures were taken to ensure the reproducibility and consistency of the specimens used in the tensile and compression tests. For this purpose, all the material and all the specimens were stored and kept under controlled temperature and humidity conditions. The sketches of both specimens are shown in Figure 2.

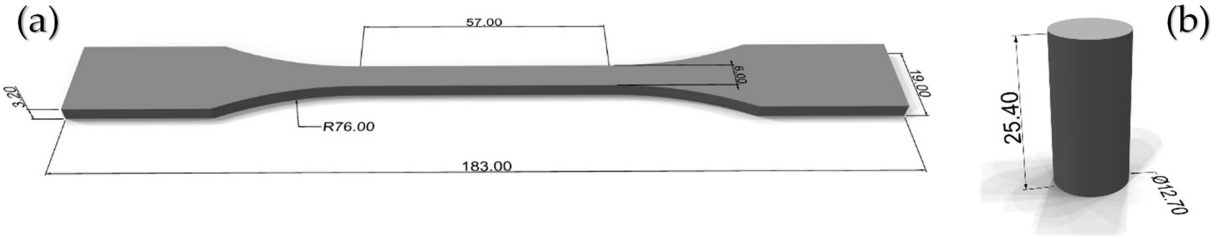

Figure 2. "Bone-type" test specimen (**a**), and cylindrical test specimen (**b**).

For the tensile and compression tests, the equipment used is the same: Shimadzu AG-X 50kN with a 50 kN maximum load cell without extensometer (Shimadzu Corporation, Kyoto, Japan), with specific tools used to perform each test.

Regarding the fabrication parameters, the layer thickness determines the vertical resolution of the printed model and the infill influences the mechanical strength of the printed model [28]. Moreover, the manufacturing temperature affects the viscosity of the

material and its adhesion to the printing bed, and can also affect the crystallinity of the material, influencing the strength and durability of the printed part [29]. Therefore, layer thickness and temperature have been selected as the process parameters. The rest of the parameters are considered to be constant, including the printing speed, which has been set to 60 mm/s as it has been estimated to be optimal in previous studies [12].

Based on previous experimental studies, a set of parameters have been considered as optimal conditions for the development of the specimens used in this research. The parameters used are shown in Table 1. Three specimens were fabricated with each parameter variation.

Table 1. Materials and manufacturing parameters.

Material	T (°C)	Layer Thickness (mm)	Extrusion Velocity (mm/s)	Overlap	Bed Temperature (°C)	Infill	Top
PETG + CF	220	0.15/0.25/0.35	60	55%	80	Concentric (100%)	Concentric
	230	0.15/0.25/0.35					
	240	0.15/0.25/0.35					

The mechanical tests were conducted using a Shimadzu AG-X 50 kN testing machine, under the control of Trapezium X 2.71 software (Shimadzu Corporation, Kyoto, Japan). The testing machine has a sensitivity of 0.01 N and a speed range spanning from 0.001 to 500 mm/min. For the case of the bone-type specimens, with a characteristic length of 135 mm, the test was carried out at a constant tensile speed of 5 mm/min. Regarding the compression tests, the cylindrical specimens of 12.7 mm diameter were initially subjected to loads at a constant compression speed of 1.3 mm/min, increasing to 5 mm/min when the elastic limit of the material was achieved, ending the test when 10 mm of deformation was reached.

Before carrying out the tests, a geometric characterization of the specimens was carried out in order to analyze possible deviations and study their possible influence on the obtained results. Likewise, a characterization by microscopy techniques was carried out before and after the tests in order to analyze the typical manufacturing defects, as well as the type of fracture that appears. The study of visual defects was carried out by SOM microscopy and focus variable microscopy technology using a Leica S9i (Leica Camera, Wetzlar, Germany) and a Bruker/Alicona Infinite Focus G5+ systems (Bruker/Alicona, Raaba, Austria), Figure 3, also used for the evaluation of Ra and Rz roughness parameters.

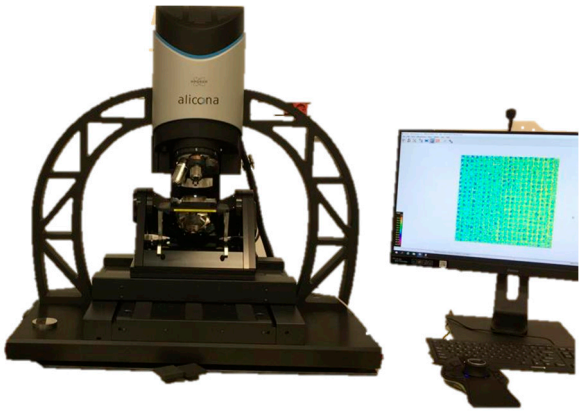

Figure 3. Focus Variable Microscopy (FVM) System for visual inspection and roughness measurement.

To evaluate the CF reinforcement effects on the friction and wear behavior, Pin-on-Disc (PoD) tests, following ASTM G99-17 Standard, have been carried out, using a MT/60/NI Microtest Tribometer (Microtest S.A., Madrid, Spain), Figure 4, and setting a 15 N load

and 250 m of sliding distance as the test conditions. AISI 316L Steel spheres with 3 mm diameter have been used as the pins. Circular specimens used as discs were developed with a concentric pattern, with the aim of avoiding the influence of the texture orientation in the coefficient of friction behavior, according to previous studies [30,31].

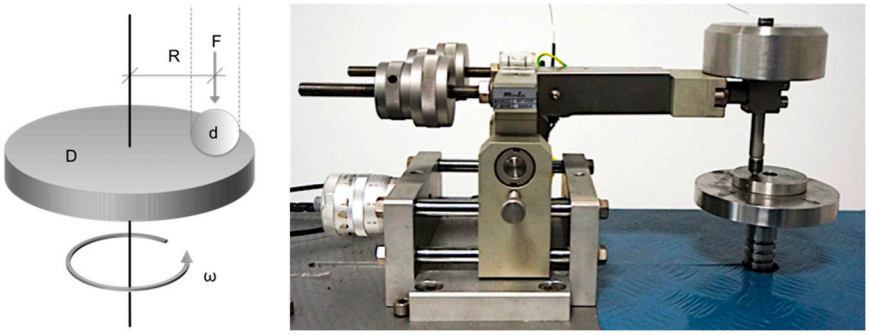

Figure 4. Pin-on-disc tribometer.

Before carrying out the tests, a geometric characterization of the specimens was carried out in order to analyze possible deviations and study their possible influence on the obtained results. Likewise, a characterization by microscopy techniques was carried out before and after the tests in order to analyze the specimens.

3. Results

Similar to other polymeric materials, PETG undergoes modifications in its properties when it reaches a certain temperature. Being a thermoplastic material, it exhibits softening and demonstrates highly viscous behavior [14,15]. This happens during the extrusion process, that is why it is very common to find some typical defects in FFF parts obtained in PETG. Consequently, as can be seen in Figure 5a,b, specimens show a tendency to accumulate material resulting in voids and porosities. In the same way, it is very common for the specimens to exhibit the formation of residual threads that need to be eliminated. Both defects are mainly due to non-homogeneous material extrusion caused by the mentioned viscosity. When CF is added, these defects are modified and accumulations appear in the trajectory changes (Figure 5c), in addition to other defects such as lack of cohesion. Figure 5d shows the reinforcement filaments and their alignment in the extrusion direction, which shows a lack of cohesion with the matrix.

In addition, viscosity impacts the potential variations in the size of the specimens. When assessing the RMS of deviations observed in the specimens (as shown in Figure 6), a noticeable trend towards increased deviation becomes evident with rising temperatures and layer thickness. This trend is observable in both the in-plane deviations (Figure 6a) and the Z-deviations (Figure 6b).

However, as observed in the case of unreinforced PETG, while the in-plane deflections are positive, the Z-deviations are negative. This phenomenon may be attributed to the flow of the molten material, causing it to spread and widen while simultaneously decreasing its height. A similar effect has been noted in various other thermoplastic materials [32]. It is noticeable that the most significant deviations occur at higher temperatures, where the material exhibits greater fluidity.

When analyzing this effect on the CF-reinforced specimens (Figure 6), it can be seen that the deviations are higher. Therefore, in this case the reinforcement induces a significant macroscopic defect, which is in agreement with what was previously observed. In this case it can also be seen that there is no clear proportionality between the deviations, although it can be seen that the increase in temperature and thickness affects the specimens negatively.

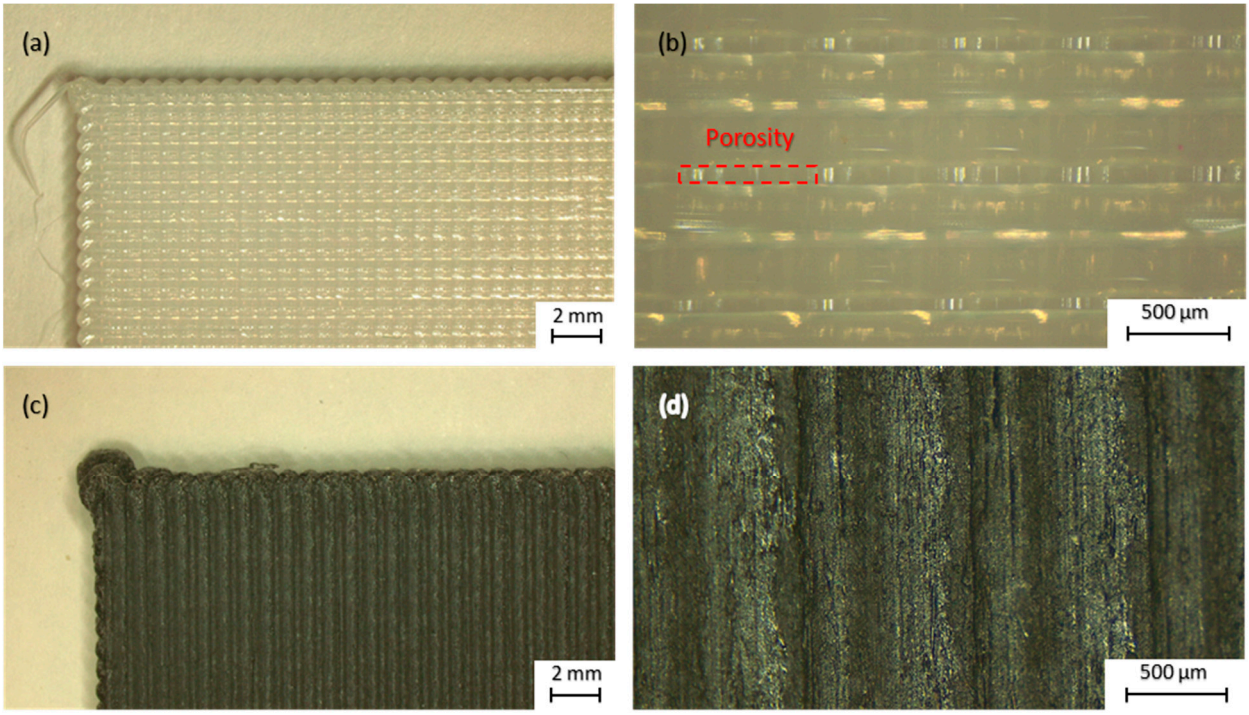

Figure 5. Defectology: (**a**) overall appearance of parts of PETG parts; (**b**) zoom of the surface texture of PETG parts; (**c**) overall appearance of CF-reinforced PETG parts; (**d**) zoom of the surface texture of CF-reinforced PETG parts.

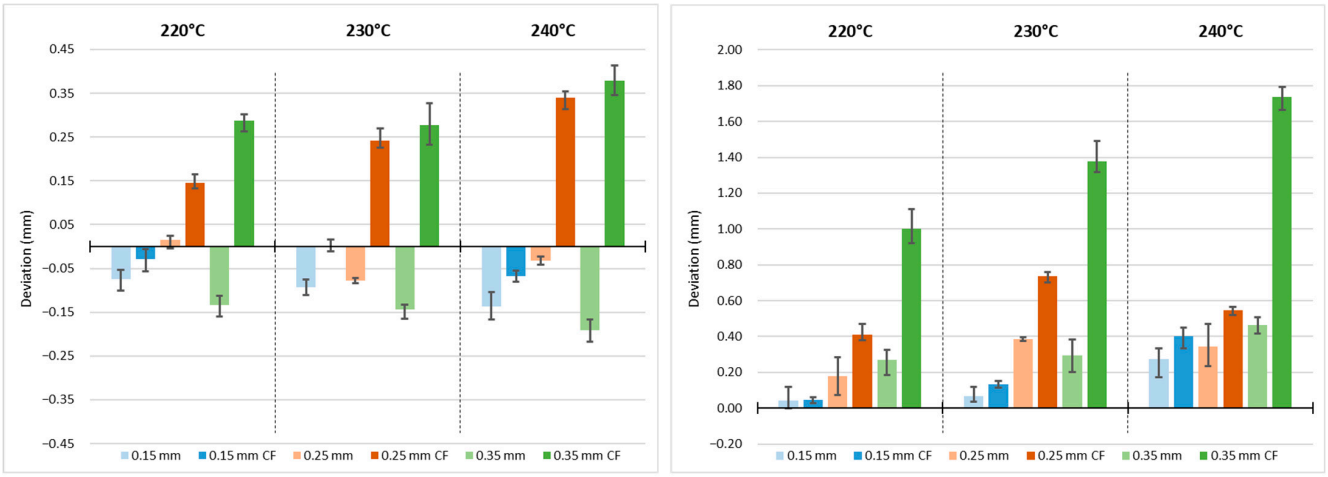

Figure 6. Dimensional deviations of PETG and PETG-CF specimens: (**a**) width and (**b**) thickness.

This may be due to the extrusion mechanism of the filament, since it must be heated and extruded by passing it through a nozzle whose lower orifice is 0.4 mm. In this way, there is a reduction in sections that can lead to the accumulation of reinforcements, which would cause a non-uniform extrusion. This effect is very common in reinforced composites [33]. Higher temperatures cause a higher fluence, but the addition of the increased layer thickness, and therefore the speed at which the material is extruded, causes greater extrusion problems.

The analysis of the extruded filaments has revealed that the addition of CF reinforcement causes an increase in the roughness of the filament surface, as shown in Figure 7. The increase in the roughness values, combined with the abrasive effect of the reinforce-

ment particles, results in an increase in the friction between the filament and the extruder. Additionally, the higher friction results in the growth of the volume of detached particles, causing wear phenomena and the obstruction of the extruder.

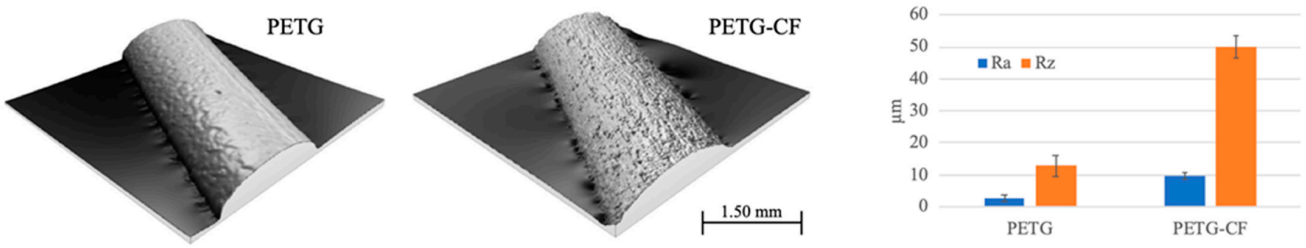

Figure 7. Roughness variation in native filaments of PETG and PETG-CF.

The challenges related to the extrusion of this material, leading to nozzle damage and premature nozzle wear due to material adhesion on the inner nozzle walls, hold significant importance. Figure 8, measured by stereoscopic microscopy techniques using Leica software, illustrates the initial section of the 1.95 mm diameter brass nozzle, which has been reduced by more than 20% due to issues related to material adhesion on the nozzle walls. This effect results in a substantial hindrance to the proper flow of the 1.75 mm diameter material, resulting in material shortages during extrusion. Furthermore, as previously discussed, the hardness of the reinforcement contributes to an abrasive effect that hinders the smooth movement of the filament through the channel and nozzle, thereby generating increased friction and subsequent difficulties in material extrusion.

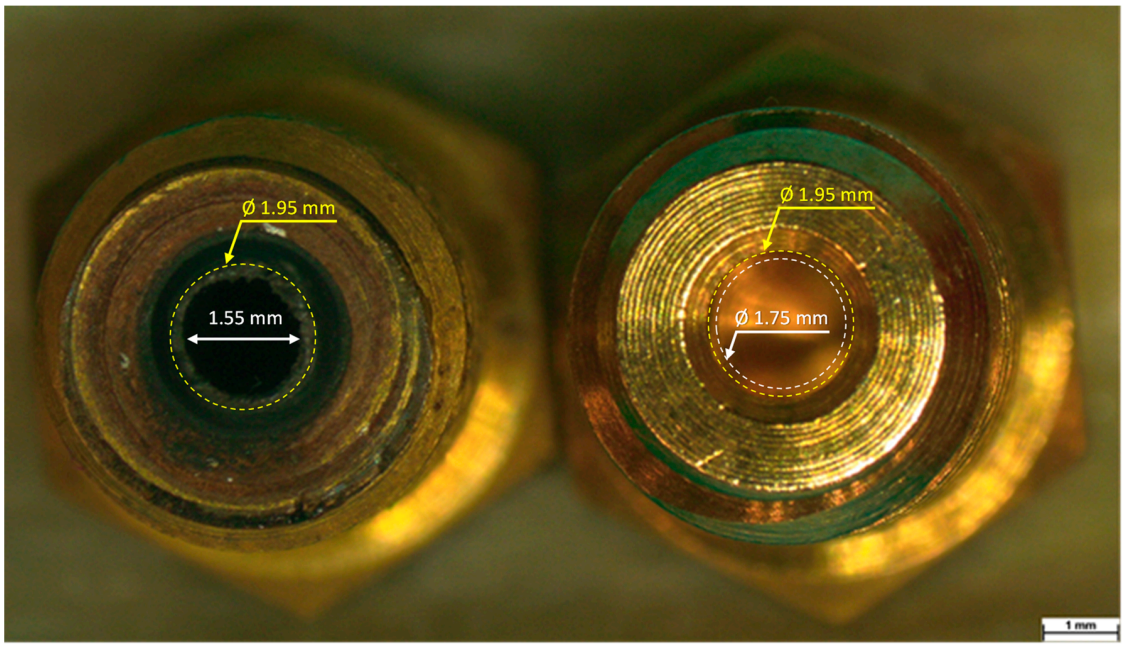

Figure 8. Worn nozzle versus new nozzle and the effective diameter measurement.

However, this is a generic problem due to the fact that the roughness of the filament is higher because of the reinforcement, which hinders the sliding and therefore causes a discontinuous fluence that can generate voids and internal porosities in the printed parts. Therefore, the hardness of the reinforcement in combination with this roughness causes alterations in the dynamic behavior of the parts. An analysis of the wear coefficient obtained with a pin-on-disc test, Figure 9, shows that PETG-CF exhibits a higher wear coefficient than the unreinforced material. Likewise, it is observed that the wear track is smaller. However, the detached material is lower in the case of PETG-CF, which may be due

to the fact that the reinforcement acts as a binder and prevents the detachment of particles. The same effect, however, may favor the accumulation of material already observed in the interior of the nozzle.

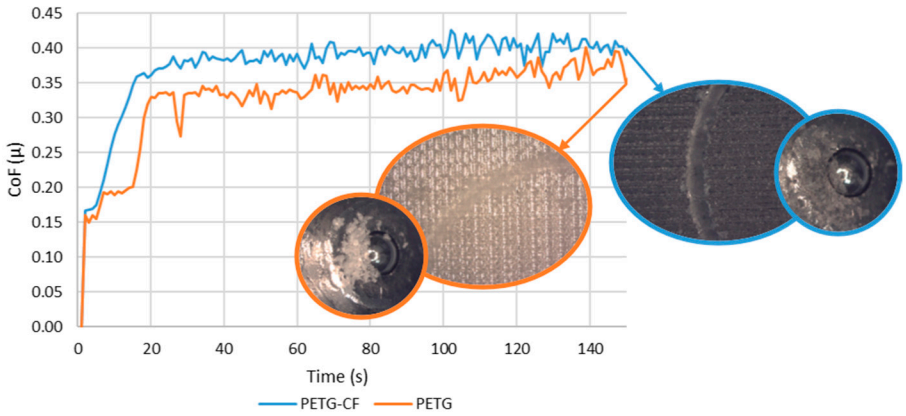

Figure 9. Comparative PoD for the 240 °C and 0.25 mm tests for PETG and PETG-CF.

These effects, which may cause difficulties in the fluence of the material, can modify the mechanical behavior of the parts subjected to stresses. Therefore, when analyzing the behavior of the specimens with the different variables studied, shown in Figures 10 and 11, it can be seen that the increase in layer thickness provides a homogenizing effect. Consequently, as the thickness increases, the dispersion of the results is smaller, i.e., the specimens become mechanically similar when the layer thickness increases. This may be due to the voids that appear between the filaments, which in the case of greater thicknesses are larger and therefore this causes the behavior of the specimen to be conditioned by this effect.

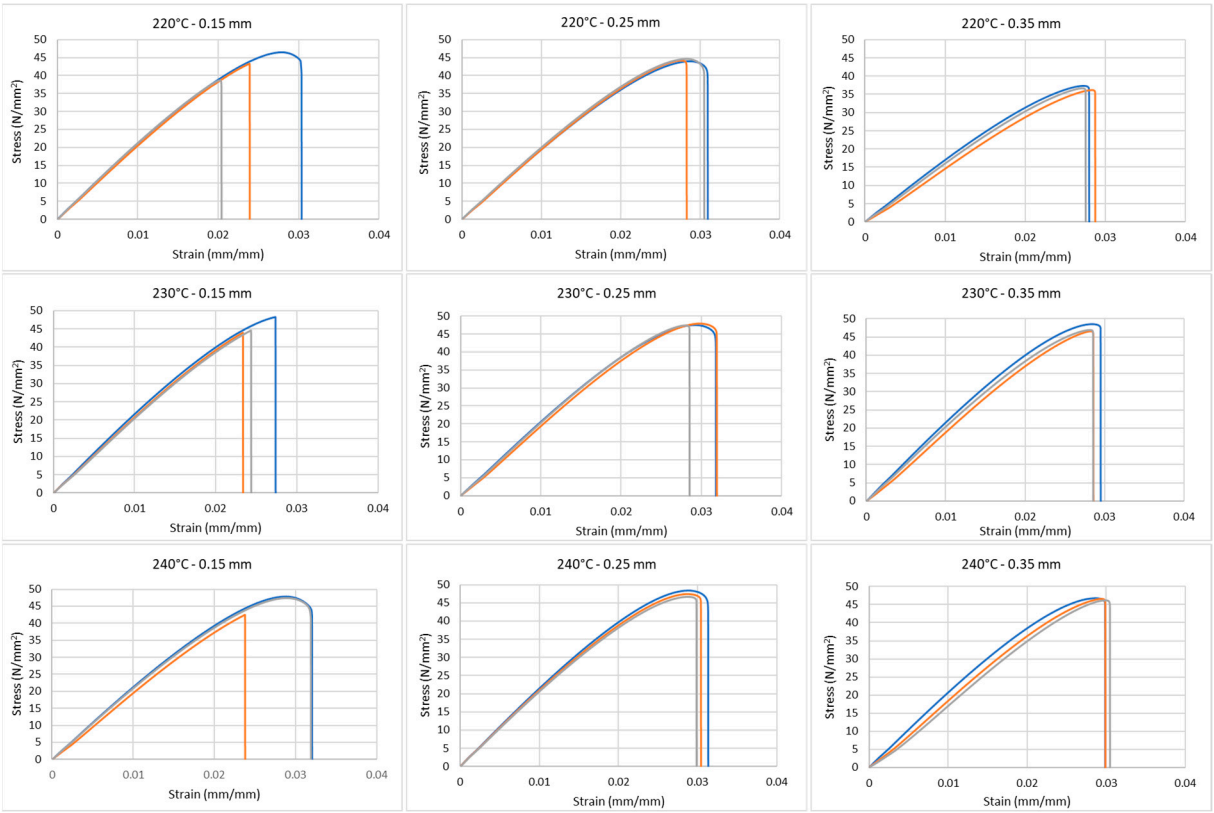

Figure 10. Tensile test results (stress–strain) for PETG material.

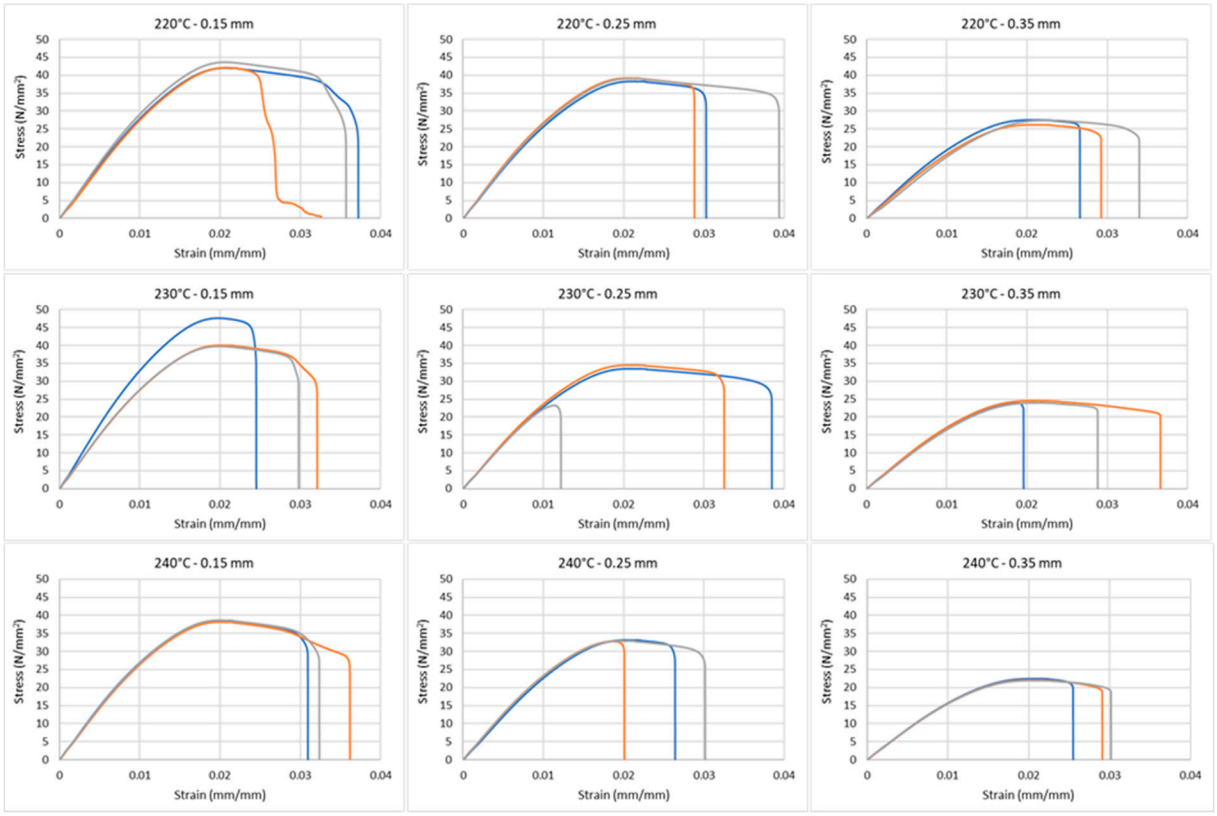

Figure 11. Results of tensile tests (stress–strain) for PETG-CF material.

Under this consideration, similar studies about mechanical properties show comparative results according to the main trends obtained in this research [34–36]. Regarding the tests with PETG-CF, as shown in Figure 11, a significantly different behavior is observed, showing a tendency of the material to reduce its performance as the layer thickness increases. As explained above, with the greater layer thickness, accentuated under the effect of the reinforcement fibers, the empty spaces between the filaments are even greater, resulting in lower cohesion between layers, which causes lower values than those in the PETG tests.

The combined data analysis (Figure 12) reveals that for PETG, the best results were achieved at the intermediate layer thickness value (0.25 mm), which exhibited the smallest Z-deviations. This is explained by the same effect: for lower layer thicknesses, the lower deformation is caused by the greater cohesion between the layers, and in higher layer heights, it is the opposite; this is presumably caused by the lower density of the part due to the increase in empty voids by the greater width of the deposited filament. Also, the tendency in the material is to stabilize at higher temperatures. However, the analysis of PETG-CF (Figure 12) shows the opposite behavior to the non-reinforced material with respect to the layer thickness, decreasing drastically as the layer thickness increases, showing a trend inversely proportional to the deviation, which allows for ensuring that these deviations cause internal defects in the parts.

When examining the fracture images of the tested specimens, a brittle fracture pattern is evident in PETG (Figure 13a), representing a failure caused by the individual filament failures within the specimen. This characteristic failure mode is distinctive in Additive Manufacturing [37–40]. However, in the case of the reinforced specimen, a more ductile failure is observed (Figure 13b), clearly influenced by the movement of the reinforcements within the material matrix. This effect might contribute to the alteration of the matrix's behavior and, consequently, result in a reduced elongation capacity due to the accumulation of reinforcements in critical zones of the specimen.

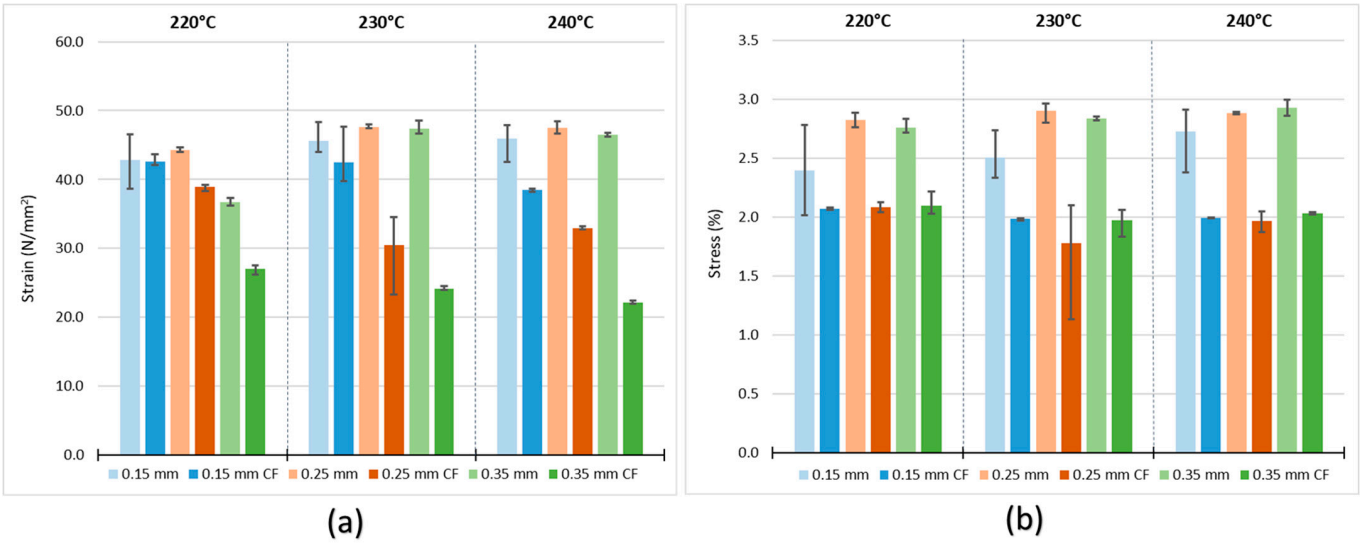

Figure 12. Mean tensile test results ((**a**) strain; (**b**) stress) for PETG and PETG-CF material.

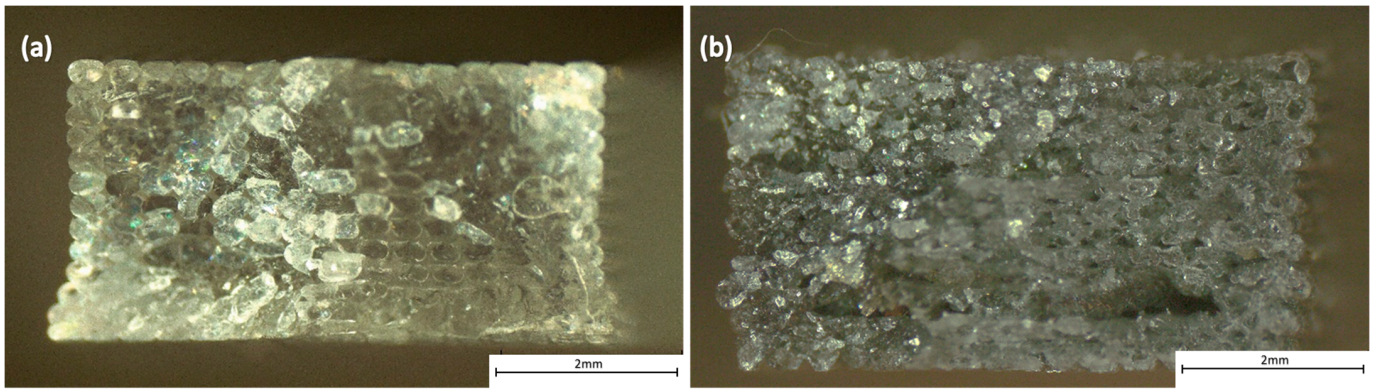

Figure 13. Fracture analysis: (**a**) PETG; (**b**) PETG-CF.

In addition, most of the fractures are located in similar positions on the tensile test specimens, Figure 14. This effect can be confirmed under each combination of printing parameters (layer thickness, temperature), ensuring the uniformity of the printing conditions and the material homogeneity through the evaluation of three repeated tensile tests.

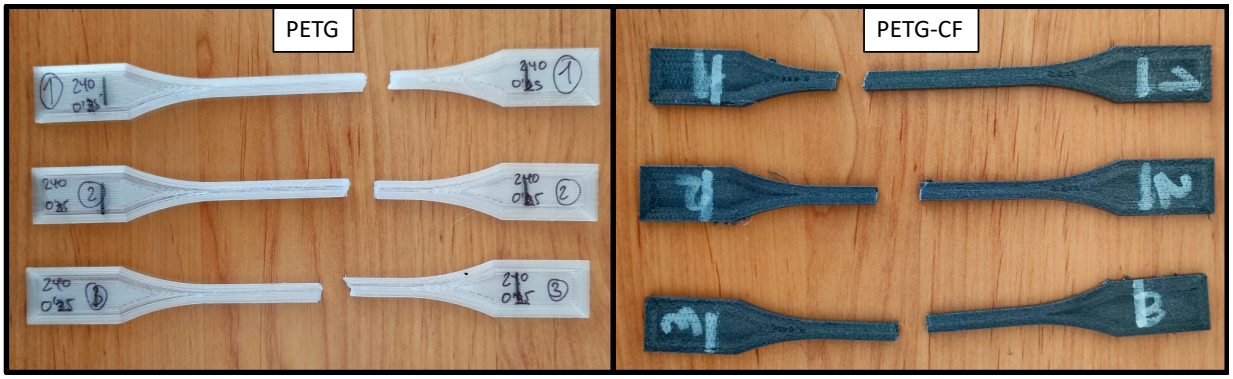

Figure 14. Fracture behavior under tensile tests for xxx conditions in PETG and PETG-CF.

A similar effect appears when the specimens are subjected to compression tests, where a strong dependence on the layer thickness appears in the case of PETG (Figure 15a). This

agrees with the study of Durgashyam et al. [16] who defined that the most influential parameter in the results is the layer thickness. It can be seen that at 0.15 mm thickness the material resists a greater stress in the elastic zone, and this decreases as the layer thickness increases. When looking at the fluence zone (or elasto-plastic transition) for the three thicknesses it seems that the change from one zone to another follows a similar pattern. However, this is not the case for the plastic zone, where the 0.15 mm thickness gives a part performance that deviates from what would be expected, decreasing drastically before it starts to grow steadily, as in the other cases. On the other hand, for the PETG-CF material (Figure 15b), the result is very similar in the elastic zone of the graph, decreasing with the increase in the thickness of the thickness used; the fluence zone is similar in the three cases, although less accentuated, predictably due to the reinforcement. The plastic zone grows steadily as the layer thickness increases, without showing a change in trend as occurs with PETG. Therefore, it can be seen that the compression result seems to be more stable in the case of PETG-CF.

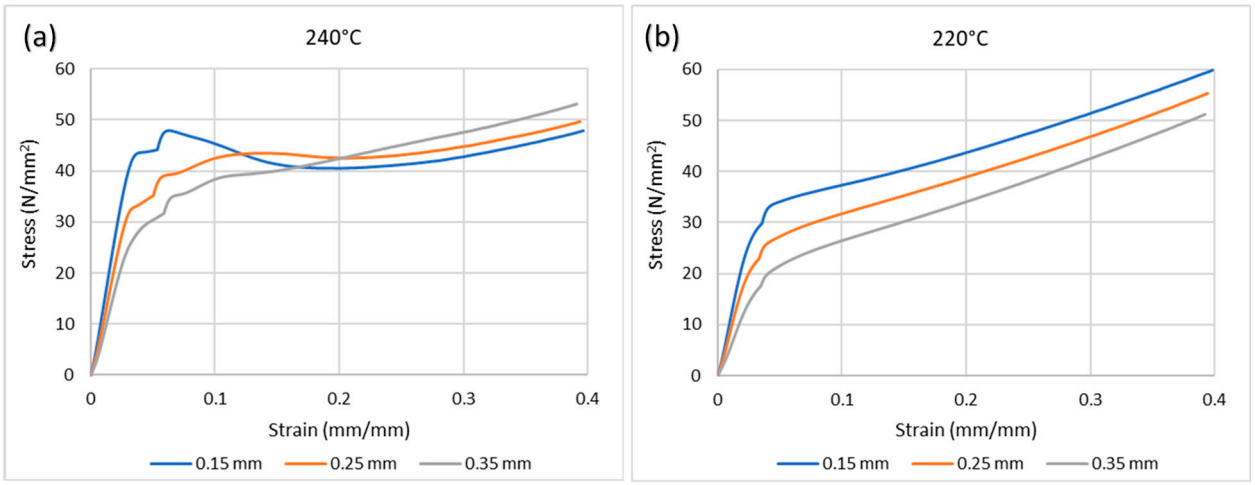

Figure 15. Compression tests (stress–strain): (**a**) PETG; (**b**) PETG-CF.

When the data are analyzed as a whole (Figure 16), it can be seen that in the case of PETG-CF, the results are more consistent and show better performance. Therefore, the incorporation of reinforcement improves certain properties, such as compression strength.

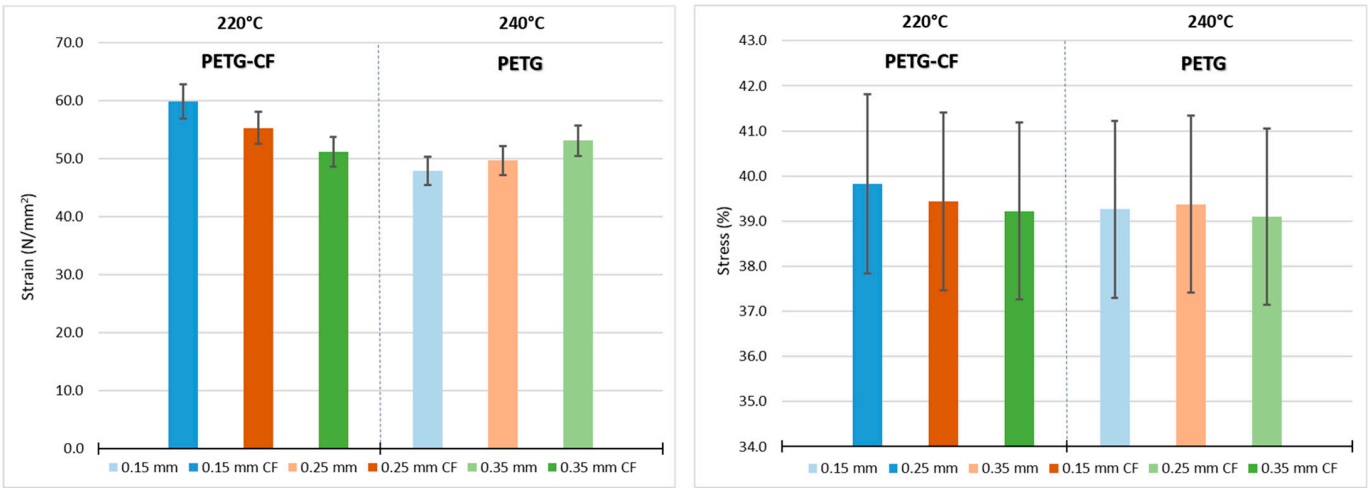

Figure 16. Maximum compression test results for PETG and PETG-CF material.

Compression tests show similar effects in both specimen types (CF-reinforced PTEG and non-reinforced PETG). The fracture of the compression test specimens has not been

detected. The deformation of the cylindrical test specimens results in the increase in the diameter size in the middle of the specimen, as shown in Figure 17.

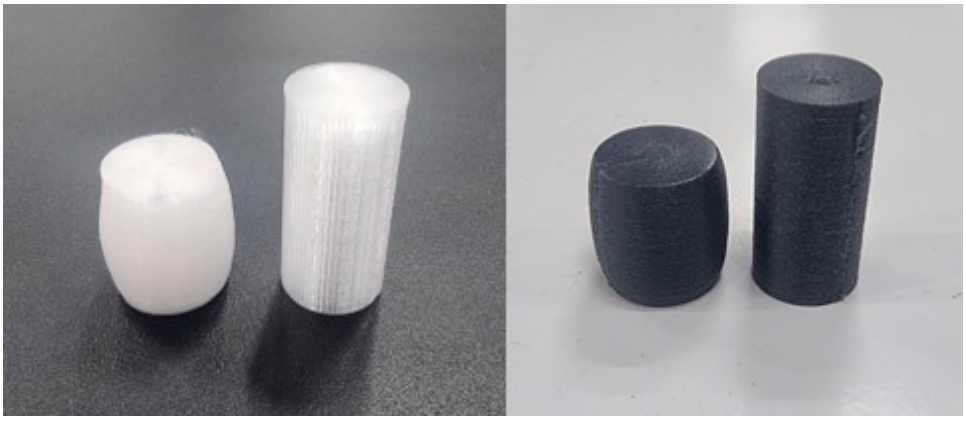

Figure 17. Compression test deformation effect for PETG and PETG-CF material.

Finally, an ANOVA analysis shown in Table 2 was carried out to determine the statistical influence of the manufacturing parameters of the specimens on the variables studied, resulting in the following considerations:

Table 2. ANOVA analysis.

	DF	Adj SC	Adj MC	F-Value	*p*-Value
Average thickness					
Model	8	0.34689	0.043361	77.66	0.000
Material	1	0.99236	0.992357	1777.26	0.000
Model-Material	8	0.43558	0.054447	97.51	0.000
Error	36	0.02010	0.000558		
Total	53	1.79492			
	DF	Adj SC	Adj MC	F-Value	*p*-Value
Average width					
Model	8	5.5941	0.69926	144.68	0.000
Material	1	2.7650	2.76504	572.08	0.000
Model-Material	8	2.5772	0.32215	66.65	0.000
Error	36	0.1740	0.00483		
Total	53	11.1103			
	DF	Adj SC	Adj MC	F-Value	*p*-Value
Thickness Deviation					
Model	8	0.34689	0.043361	77.66	0.000
Material	1	0.99236	0.992357	1777.26	0.000
Model-Material	8	0.43558	0.054447	97.51	0.000
Error	36	0.02010	0.000558		
Total	53	1.79492			
	DF	Adj SC	Adj MC	F-Value	*p*-Value
Width Deviation					
Model	8	5.5941	0.69926	144.68	0.000
Material	1	2.7650	2.76504	572.08	0.000
Model-Material	8	2.5772	0.32215	66.65	0.000
Error	36	0.1740	0.00483		
Total	53	11.1103			

Table 2. *Cont.*

	DF	Adj SC	Adj MC	F-Value	*p*-Value
Force					
Model	8	90,846	11,356	6.14	0.000
Material	1	407,554	407,554	220.51	0.000
Model-Material	8	123,841	15,480	8.38	0.000
Error	36	66,535	1848		
Total	53	688,776			
	DF	Adj SC	Adj MC	F-Value	*p*-Value
Displacement					
Model	8	0.6778	0.0847	1.29	0.277
Material	1	13.9657	13.9657	213.40	0.000
Model-Material	8	1.2086	0.1511	2.31	0.041
Error	36	2.3559	0.0654		
Total	53	18.2080			
	DF	Adj SC	Adj MC	F-Value	*p*-Value
Stress					
Model	8	842.7	105.33	20.43	0.000
Material	1	1848.8	1848.80	358.58	0.000
Model-Material	8	899.7	112.46	21.81	0.000
Error	36	185.6	5.16		
Total	53	3776.7			
	DF	Adj SC	Adj MC	F-Value	*p*-Value
Strain					
Model	8	0.3719	0.04649	1.29	0.277
Material	1	7.6629	7.66293	213.40	0.000
Model-Material	8	0.6631	0.08289	2.31	0.041
Error	36	1.2927	0.03591		
Total	53	9.9906			

ANOVA analysis showing the statistical influence of texturing parameters on surface quality parameters Sa, Sz, and Sk.

When analyzing Average Thickness, Average Width, Thickness Deviation, Width Deviation, Force, Displacement, Stress, and Strain against Test Variables and the incorporation of reinforcement, a high statistical significance is observed for both test variables (specimen manufacturing parameters) and the use of reinforcement in all parameters, with a significant influence of reinforcement, except in the case of displacement and strain, where the *p*-value indicates no significance of the test parameters.

When analyzing Average Thickness, Average Width, Thickness Deviation, Width Deviation, Force, Displacement, Stress, and Strain against Extrusion Temperature, Layer Thickness, and the incorporation of reinforcement, it is observed that for thickness and thickness deviation, temperature has no significance, while layer thickness has much significance, with the influence of layer thickness highly conditioned by the reinforcement due to the interaction of the two factors and their F-value. For width and width deviation, all values have significance, but in this case, temperature is much less significant than layer thickness, and reinforcement incorporation has less influence.

Regarding mechanical parameters (Force, Displacement, Stress, and Strain), none seem to be affected by temperature. Similarly, only stress is affected by the interaction of temperature and layer thickness. In all cases, there is a very significant influence of reinforcement incorporation, although in the case of displacement and strain, there is no significance in the case of the interaction between temperature and reinforcement.

4. Conclusions

According to the results of the tensile tests, the incorporation of carbon fiber reinforcement has a detrimental effect, leading to a decrease in the maximum stress (834.052 N compared to 956.6 N for conventional PETG) and a reduction in the material's strength (39.23 N/mm^2 vs. 48.41 N/mm^2 for the conventional material). As expected, due to the nature of the reinforcement (short fibers), the deformation of the material also decreases (2.13% compared to 2.9%). Therefore, it may not be suitable for applications requiring high ductility in tensile strength.

Conversely, conventional PETG appears to be a more attractive option for applications involving tensile stresses. It demonstrates improved performance at higher temperatures, and the best results are obtained at medium layer thicknesses (0.25 mm), despite the potential expectation of increased layer cohesion at lower thicknesses.

The compression tests reveal distinct behaviors in both materials, with the reinforced material outperforming the non-reinforced material, as anticipated. In the case of the standard material, increasing the layer thickness leads to better results across all relevant variables. In contrast, for the reinforced material, improved results are achieved as layer thickness decreases due to increased layer cohesion.

In the context of the compressive tests, it is evident that the displacement and the deformation are considerably lower with the minimum layer thickness used for conventional PETG. This could be attributed to the absence of internal voids that may have been introduced by the reinforcement in the PETG matrix.

Considering the dimensional deviations calculated for the specimens, a clear trend emerges where the material stabilizes at medium layer thicknesses. In terms of tensile strength, the positive deviation benefits the conventional material, but not the reinforced one. Additionally, it is observed that thinner layer thicknesses result in a more fragile rupture due to the increased cohesion between layers, especially in the case of the conventional material. However, this is not the case for the reinforced material, where the tensile results are most favorable for the thinner layer thickness. Even though there is a negative deviation in both measured dimensions, it yields the highest mechanical performance.

In conclusion, the incorporation of CF reinforcement into the PETG matrix is beneficial for applications involving compressive strength but not tensile strength, where conventional PETG is the preferred material. The results confirm that, as reported by several authors, layer thickness is the most critical parameter influencing the material's behavior in both test cases.

Author Contributions: Conceptualization, J.M.L., J.M.V.-M. and M.B.; project administration, M.R.-P.; experimental methodology, J.M.L.; investigation, J.M.V.-M. and M.B.; data processing, J.M.L.; formal analysis, J.M.L., J.M.V.-M. and M.B.; project review, M.R.-P.; writing—original draft preparation, J.M.L. and M.B.; writing—review and editing, J.M.V.-M.; final review, M.R.-P. All authors have read and agreed to the published version of the manuscript.

Funding: This research received no external funding.

Institutional Review Board Statement: Not applicable.

Informed Consent Statement: Not applicable.

Data Availability Statement: Data are contained within the article.

Acknowledgments: This work has been developed under the support of the Mechanical Engineering and Industrial Design department and the Vice-Rector's Office for Scientific Policy of the University of Cadiz.

Conflicts of Interest: The authors declare no conflict of interest.

References

1. Huang, Y.; Leu, M.C.; Mazumder, J.; Donmez, A. Additive Manufacturing: Current State, Future Potential, Gaps and Needs, and Recommendations. *J. Manuf. Sci. Eng.* **2015**, *137*, 014001. [CrossRef]
2. Dey, A.; Roan Eagle, I.N.; Yodo, N. A Review on Filament Materials for Fused Filament Fabrication. *J. Manuf. Mater. Process.* **2021**, *5*, 69. [CrossRef]
3. Kechagias, J.D.; Ninikas, K.; Petousis, M.; Vidakis, N.; Vaxevanidis, N. An investigation of surface quality characteristics of 3D printed PLA plates cut by CO_2 laser using experimental design. *Mater. Manuf. Process.* **2021**, *36*, 1544–1553. [CrossRef]
4. Kechagias, J.D.; Chaidas, D.; Vidakis, N.; Salonitis, K.; Vaxevanidis, N.M. Key parameters controlling surface quality and dimensional accuracy: A critical review of FFF process. *Mater. Manuf. Process.* **2022**, *37*, 963–984. [CrossRef]
5. Mushtaq, R.T.; Iqbal, A.; Wang, Y.; Khan, A.M.; Petra, M.I. Advancing PLA 3D printing with laser polishing: Improving mechanical strength, sustainability, and surface quality. *Crystals* **2023**, *13*, 626. [CrossRef]
6. Mushtaq, R.T.; Iqbal, A.; Wang, Y.; Khan, A.M.; Bakar, M.S.A. Parametric optimization of 3D printing process hybridized with laser-polished PETG polymer. *Polym. Test.* **2023**, *125*, 108129. [CrossRef]
7. Mushtaq, R.T.; Wang, Y.; Khan, A.M.; Rehman, M.; Li, X.; Sharma, S. A post-processing laser polishing method to improve process performance of 3D printed new Industrial Nylon-6 polymer. *J. Manuf. Process.* **2023**, *101*, 546–560. [CrossRef]
8. Ngo, T.D.; Kashani, A.; Imbalzano, G.; Nguyen, K.T.; Hui, D. Additive manufacturing (3d printing): A review of materials, methods, applications and challenges. *Compos. Part B Eng.* **2018**, *143*, 172–196. [CrossRef]
9. Dupaix, R.B.; Boyce, M.C. Finite strain behavior of poly (ethylene terephthalate) (PET) and poly (ethylene terephthalate)-glycol (PETG). *Polymer* **2005**, *46*, 4827–4838. [CrossRef]
10. Dupaix, R.B.; Krishnan, D. A Constitutive Model for Strain-Induced Crystallization in Poly (ethylene terephthalate) (PET) during Finite Strain Load-Hold Simulations. *J. Eng. Mater. Technol.* **2005**, *128*, 28–33. [CrossRef]
11. Vikneswaran, S.K.; Nagarajan, P.; Dinesh, S.K.; Senthil Kumar, K.L.; Megalingam, A. Investigation of the tensile behaviour of Polylactic Acid, Acrylonitrile Butadiene Styrene, and Polyethylene Terephthalate Glycol materials. *Mater. Today Proc.* **2022**, *66*, 1093–1098. [CrossRef]
12. Valvez, S.; Silva, A.P.; Reis, P.N.B. Optimization of Printing Parameters to Maximize the Mechanical Properties of 3D-Printed PETG-Based Parts. *Polymers* **2022**, *14*, 2564. [CrossRef] [PubMed]
13. Dolzyk, G.; Jung, S. Tensile and Fatigue Analysis of 3D-Printed Polyethylene Terephthalate Glycol. *J. Fail. Anal. Prev.* **2019**, *19*, 511–518. [CrossRef]
14. Hsueh, M.H.; Lai, C.J.; Wang, S.H.; Zeng, Y.S.; Hsieh, C.H.; Pan, C.Y.; Huang, W.C. Effect of Printing Parameters on the Thermal and Mechanical Properties of 3D-Printed PLA and PETG, Using Fused Deposition Modeling. *Polymers* **2021**, *13*, 1758. [CrossRef] [PubMed]
15. Grasso, M.; Azzouz, L.; Ruiz-Hincapie, P.; Zarrelli, M.; Ren, G. Effect of temperature on the mechanical properties of 3D-printed PLA tensile specimens. *Rapid Prototyp. J.* **2018**, *24*, 1337–1346. [CrossRef]
16. Durgashyam, K.; Indra Reddy, M.; Balakrishna, A.; Satyanarayana, K. Experimental investigation on mechanical properties of PETG material processed by fused deposition modeling method. *Mater. Today Proc.* **2019**, *18*, 2052–2059. [CrossRef]
17. Travieso-Rodriguez, J.A.; Jerez-Mesa, R.; Llumà, J.; Traver-Ramos, O.; Gomez-Gras, G.; Roa Rovira, J.J. Mechanical Properties of 3D-Printing Polylactic Acid Parts subjected to Bending Stress and Fatigue Testing. *Materials* **2019**, *12*, 3859. [CrossRef] [PubMed]
18. Gomez-Gras, G.; Jerez-Mesa, R.; Travieso-Rodriguez, J.A.; Lluma-Fuentes, J. Fatigue performance of fused filament fabrication PLA specimens. *Mater. Des.* **2018**, *140*, 278–285. [CrossRef]
19. Wendt, C.; Fernández-Vidal, S.R.; Gómez-Parra, A.G.; Batista, M.; Marcos, M. Processing and Quality Evaluation of Additive Manufacturing Monolayer Specimens. *Adv. Mater. Sci. Eng.* **2016**, *2016*, 5780693. [CrossRef]
20. Mansour, M.; Tsongas, K.; Tzetzis, D.; Antoniadis, A. Mechanical and Dynamic Behavior of Fused Filament Fabrication 3D Printed Polyethylene Terephthalate Glycol Reinforced with Carbon Fibers. *Polym.-Plast. Technol. Eng.* **2018**, *57*, 1715–1725. [CrossRef]
21. Valvez, S.; Silva, A.P.; Reis, P.N.B. Compressive Behaviour of 3D-Printed PETG Composites. *Aerospace* **2022**, *9*, 124. [CrossRef]
22. Kasmi, S.; Ginoux, G.; Allaoui, S.; Alix, S. Investigation of 3D printing strategy on the mechanical performance of coextruded continuous carbon fiber reinforced PETG. *J. Appl. Polym. Sci.* **2021**, *138*, 50955. [CrossRef]
23. Bex, G.J.P.; Ingenhut, B.L.J.; Ten Cate, T.; Sezen, M.; Ozkoc, G. Sustainable approach to produce 3D-printed continuous carbon fiber composites: "A comparison of virgin and recycled PETG". *Polym. Compos.* **2021**, *42*, 4253–4264. [CrossRef]
24. Latko-Durałek, P.; Dydek, K.; Boczkowska, A. Thermal, Rheological and Mechanical Properties of PETG/rPETG Blends. *J. Polym. Environ.* **2019**, *27*, 2600–2606. [CrossRef]
25. Kumar, K.S.; Soundararajan, R.; Shanthosh, G.; Saravanakumar, P.; Ratteesh, M. Augmenting effect of infill density and annealing on mechanical properties of PETG and CFPETG composites fabricated by FDM. *Mater. Today Proc.* **2021**, *45*, 2186–2191. [CrossRef]
26. Alarifi, I.M. Mechanical properties and numerical simulation of FDM 3D printed PETG/Carbon composite unit structures. *J. Mater. Res. Technol.* **2023**, *23*, 656–669. [CrossRef]
27. Alarifi, I.M. PETG/carbon fiber composites with different structures produced by 3D printing. *Polym. Test.* **2023**, *120*, 107949. [CrossRef]
28. *ASTM D638-14*; Standard Test Method for Tensile Properties of Plastics. ASTM International: West Conshohocken, PA, USA, 2022.
29. *ASTM D695-15*; Standard Test Method for Compressive Properties of Rigid Plastics. ASTM International: West Conshohocken, PA, USA, 2023.

30. Batista, M.; del Sol, I.; Salguero, J.; Piñero, D.; Vázquez, J.M. Product Design: Study of the Tribological Properties of FDM PETG Products. In *Advances in Design Engineering III, INGEGRAF 2022. Lecture Notes in Mechanical Engineering*; Springer: Cham, Switzerland, 2023.
31. Batista, M.; Blanco, D.; del Sol, I.; Piñero, D.; Vazquez-Martínez, J.M. Tribological characterization of Fused Deposition Modelling parts. *IOP Conf. Ser. Mater. Sci. Eng.* **2021**, *1193*, 012068. [CrossRef]
32. Yadav, A.; Chauhan, P.; Babbar, A.; Kumar, R.; Ranjan, N.; Chohan, J.; Kumar, R.; Gupta, M. Fused filament fabrication: A state-of-the-art review of the technology, materials, properties and defects. *Int. J. Interact. Des. Manuf.* **2022**, *17*, 2867–2889. [CrossRef]
33. Tran, T.Q.; Ng, F.L.; Kai, J.T.Y.; Feih, S.; Nai, M.L.S. Tensile Strength Enhancement of Fused Filament Fabrication Printed Parts: A Review of Process Improvement Approaches and Respective Impact. *Addit. Manuf.* **2022**, *54*, 102724. [CrossRef]
34. Lu, Z.; Feng, B.; Loh, C. Fatigue behavior and mean stress effect on thermoplastic polymers and composites. *Frat. Ed Integrità Strutt.* **2018**, *46*, 150–157. [CrossRef]
35. Rodriguez, J.G.D.; Comas, A.D.P.; Herrera, J.D.S. Notch sensitivity study in u-notched polymers built by Additive Manufacturing (AM). *Frat. Ed Integrità Strutt.* **2023**, *66*, 127–139. [CrossRef]
36. Moradi, M.; Rezayat, M.; Rozhbiany, F.A.R.; Meiabadi, S.; Casalino, G.; Shamsborhan, M.; Bijoy, A.; Chakkingal, S.; Lawrence, M.; Mohammed, N.; et al. Correlation between Infill Percentages, Layer Width, and Mechanical Properties in Fused Deposition Modelling of Poly-Lactic Acid 3D Printing. *Machines* **2023**, *11*, 950. [CrossRef]
37. Valerga, A.P.; Batista, M.; Salguero, J.; Girot, F. Influence of PLA Filament Conditions on Characteristics of FDM Parts. *Materials* **2018**, *11*, 1322. [CrossRef] [PubMed]
38. Jiang, Y.; Wu, J.; Leng, J.; Cardon, L.; Zhang, J. Reinforced and toughened PP/PS composites prepared by Fused Filament Fabrication (FFF) with in-situ microfibril and shish-kebab structure. *Polymer* **2020**, *186*, 121971. [CrossRef]
39. García, E.; Núñez, P.J.; Caminero, M.A.; Chacón, J.M.; Kamarthi, S. Effects of carbon fibre reinforcement on the geometric properties of PETG-based filament using FFF additive manufacturing. *Compos. Part B Eng.* **2022**, *235*, 109766. [CrossRef]
40. Djokikj, J.; Tuteski, O.; Doncheva, E.; Hadjieva, B. Experimental investigation on mechanical properties of FFF parts using different materials. *Procedia Struct. Integr.* **2022**, *41*, 670–679. [CrossRef]

Disclaimer/Publisher's Note: The statements, opinions and data contained in all publications are solely those of the individual author(s) and contributor(s) and not of MDPI and/or the editor(s). MDPI and/or the editor(s) disclaim responsibility for any injury to people or property resulting from any ideas, methods, instructions or products referred to in the content.